

# Influence of Selenium-containing Additives on the Electrodeposition Of Zinc-Manganese Alloys

by B. Bozzini, E. Griskonis, A. Sulcius & P.L. Cavallotti

In the present paper we report on the influence of some selenium-containing additives on the electrodeposition of zinc-manganese alloys. Selenous acid (0.05–0.20 g/L) and ammonium selenate (0.5–2.0 g/L) were added to sulfate-citrate baths. Investigations of alloy composition were carried out by atomic absorption spectrometry and EDX. The morphology of the coatings was studied by SEM and the crystal structure of the as-plated and corroded samples were investigated by XRD. The effects of deposition time on quality and composition of alloy were highlighted. Corrosion behavior of Zn-Mn alloys with and without traces of selenium was investigated by measurement of free corrosion potentials in aerated sodium chloride solution.

Zinc and its alloys are often used to protect steel against corrosion. Zinc-manganese alloys show better

corrosion resistance than the individual metals.<sup>1</sup> Zinc-manganese alloy coatings can be electrodeposited from a sulfate bath,<sup>2</sup> from a sulfate bath containing citrates<sup>3-9</sup> and from a fluoborate bath.<sup>10</sup> The sulfate-citrate bath is the one used most for the electrodeposition of high-manganese Zn-Mn alloys. Baths free of organic complexing agents were developed for low-manganese automotive applications.<sup>11</sup> Variations of bath composition, temperature, pH and current density affect manganese content in terms of the alloy, current efficiency, quality and appearance of the coatings.<sup>3-9</sup> It was reported that small concentrations of some additives in the bath influence the alloy electrodeposition process.<sup>8,9</sup>

The aim of this work is to elucidate the influence of  $H_2SeO_3$  and  $(NH_4)_2SeO_4$  additions to the sulfate-citrate bath on the composition, crystal structure and morphology of Zn-Mn alloy coatings. Selenium

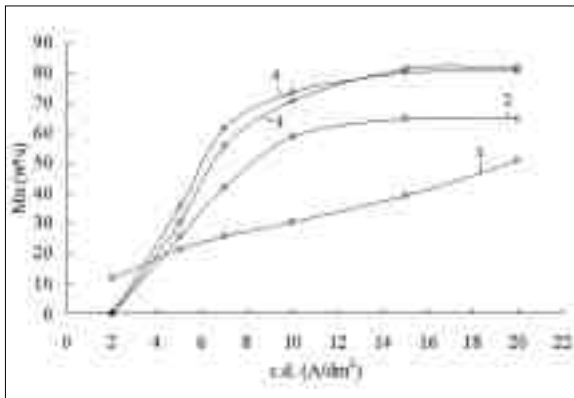


Fig. 1(a)—Effect of ammonium selenate additions on manganese content: (1) 0.0 g/L, (2) 0.5 g/L, (3) 1.0 g/L, (4) 2.0 g/L.

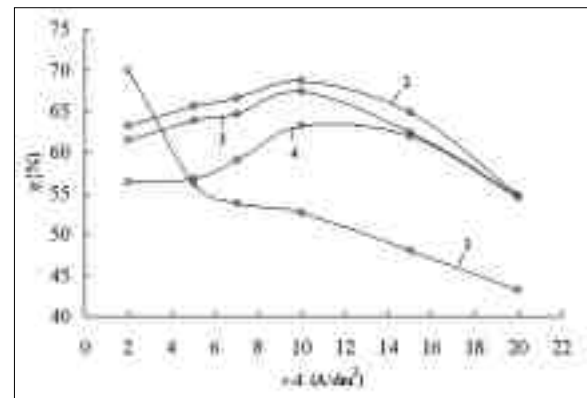


Fig. 1(c)—Effect of ammonium selenate additions on current efficiency: (1) 0.0 g/L, (2) 0.5 g/L, (3) 1.0 g/L, (4) 2.0 g/L.

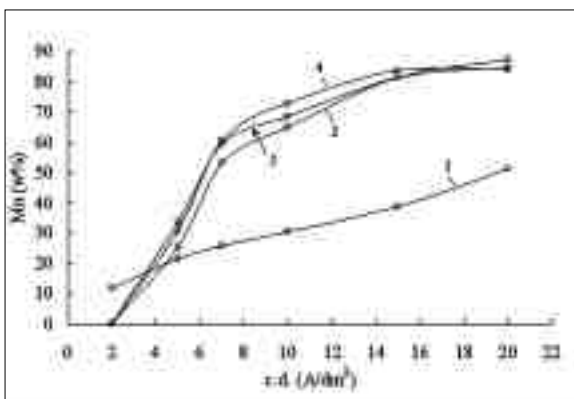


Fig. 1(b)—Effect of selenous acid additions on manganese content: (1) 0.0 g/L, (2) 0.05 g/L, (3) 0.1 g/L, (4) 0.2 g/L.

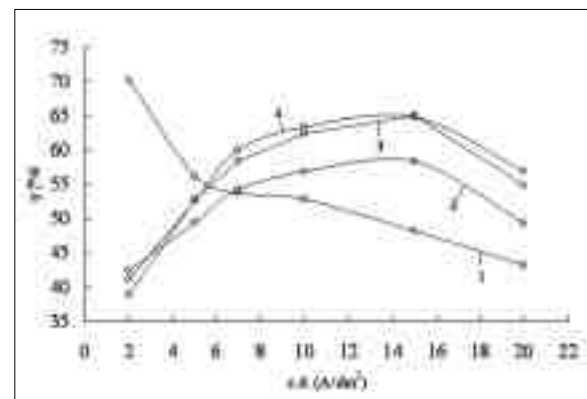


Fig. 1(d)—Effect of selenous acid additions on current efficiency: (1) 0.0 g/L, (2) 0.05 g/L, (3) 0.1 g/L, (4) 0.2 g/L.

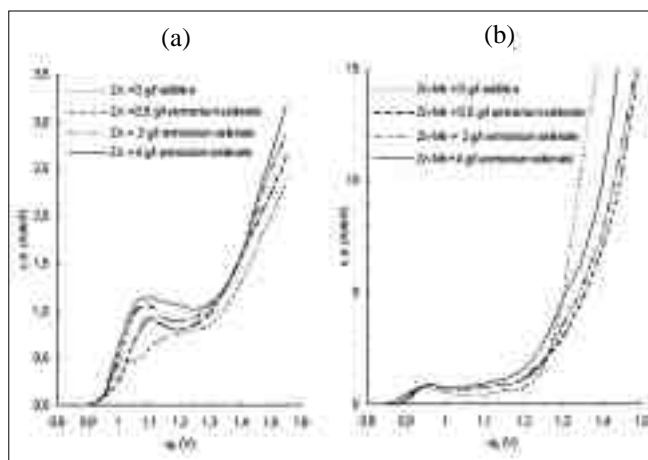


Fig. 2—Effect of ammonium selenate additions on the polarization behavior of (a) zinc and (b) Zn-Mn baths.

compounds were chosen since the effects of selenium on the kinetics of hydrogen evolution on zinc cathodes are well known.<sup>12</sup> A suppression of zinc deposition was expected which could enhance the manganese content in the coatings. There was a concern that this effect could be achieved at the expense of the deposit quality, since enhanced hydrogen evolution can induce morphological alterations. In particular, deposit properties depend on the thickness of the deposits. Therefore the achievement of high quality coatings relies on the identification of an optimal thickness range.

### Experimental Procedure

Analytical grade reagents were used. The Zn-Mn alloy electrodeposition was carried out using the following sulfate-citrate bath:

0.18 M ZnSO<sub>4</sub>  
 0.65 M MnSO<sub>4</sub>  
 0.72 M Na<sub>3</sub>C<sub>6</sub>H<sub>5</sub>O<sub>7</sub>  
 pH = 5.3  
 T = 30°C (87°F)  
 Agitation = none

Small amounts of selenous acid (H<sub>2</sub>SeO<sub>3</sub>) and ammonium selenate [(NH<sub>4</sub>)<sub>2</sub>SeO<sub>4</sub>] were added to the plating bath. Lead alloy plates containing 1% silver, coated with a MnO<sub>2</sub> film were used as anodes. The cathodes were 20 mm x 20 mm squares of carbon steel (C = 0.22%, Mn = 0.5%, Si = 0.1%, P < 0.04%, S < 0.05%) plates.

In the electrodeposition cell cathodic and anodic compartments were separated by a PVC fabric diaphragm. Polarization curves were recorded at a scan rate of 200 mV/min. The reference electrode was Ag/AgCl. The potentials are expressed versus the standard hydrogen electrode (SHE). Investigation of the composition of the Zn-Mn alloy coatings was carried out by atomic absorption spectrometry and EDX. Free corrosion potentials were measured in aerated 3% NaCl solution (T = 20°C, pH 6.4). The crystal structures of the as-plated and corroded samples were investigated by X-ray diffraction (XRD) with a powder diffractometer, and the coating morphology was studied by scanning electron microscopy (SEM).

### Results

#### Alloy Composition & Cathode Efficiency

The positive correlation of manganese content with current density, observed in all experiments, is quite typical for

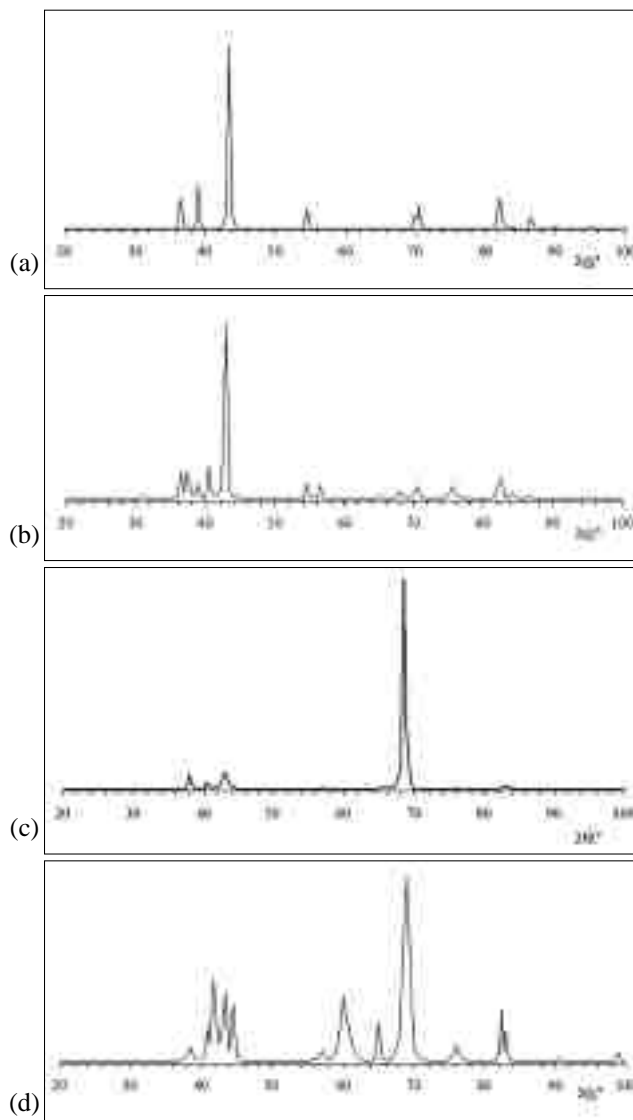


Fig. 3—X-ray diffractograms of deposits from baths containing ammonium selenate additions: (a) Current density = 2 A/dm<sup>2</sup> (20 A/ft<sup>2</sup>); (b) No (NH<sub>4</sub>)<sub>2</sub>SeO<sub>4</sub>; current density = 10 A/dm<sup>2</sup> (100 A/ft<sup>2</sup>); (c) Current density 10 A/dm<sup>2</sup> (100 A/ft<sup>2</sup>), 9 min; (d) Current density 10 A/dm<sup>2</sup> (100 A/ft<sup>2</sup>), 3 min.

a regular codeposition system such as the one at hand. It was found that small additions of selenous acid (H<sub>2</sub>SeO<sub>3</sub>) (0.05–0.20 g/L) and ammonium selenate [(NH<sub>4</sub>)<sub>2</sub>SeO<sub>4</sub>] (0.5–2.0 g/L) to the bath influenced the electrodeposition of Zn-Mn alloys. Both additives had a similar effect. The addition of the selenium compounds markedly increased the manganese content in the coatings (Figs. 1a and b) and the current efficiency (Figs. 1c and d) with cathodic current densities in the 5–20 A/dm<sup>2</sup> (50–200 A/ft<sup>2</sup>) range. At 2.0 A/dm<sup>2</sup> (20 A/ft<sup>2</sup>), the coatings obtained from the selenium-containing solution contained no manganese. Those deposited from the bath without additives contained about 12% Mn.

Local EDX analysis showed that the manganese content was higher on the tops of surface bumps or dendrites and lower in the recesses. This can be easily explained in terms of local current densities. This effect would lead to unwieldy averaging effects if the EDX analyses were carried out on surfaces with several morphological features.

Zinc-manganese alloys from plating baths containing the selenium additives contained very limited amounts of selenium

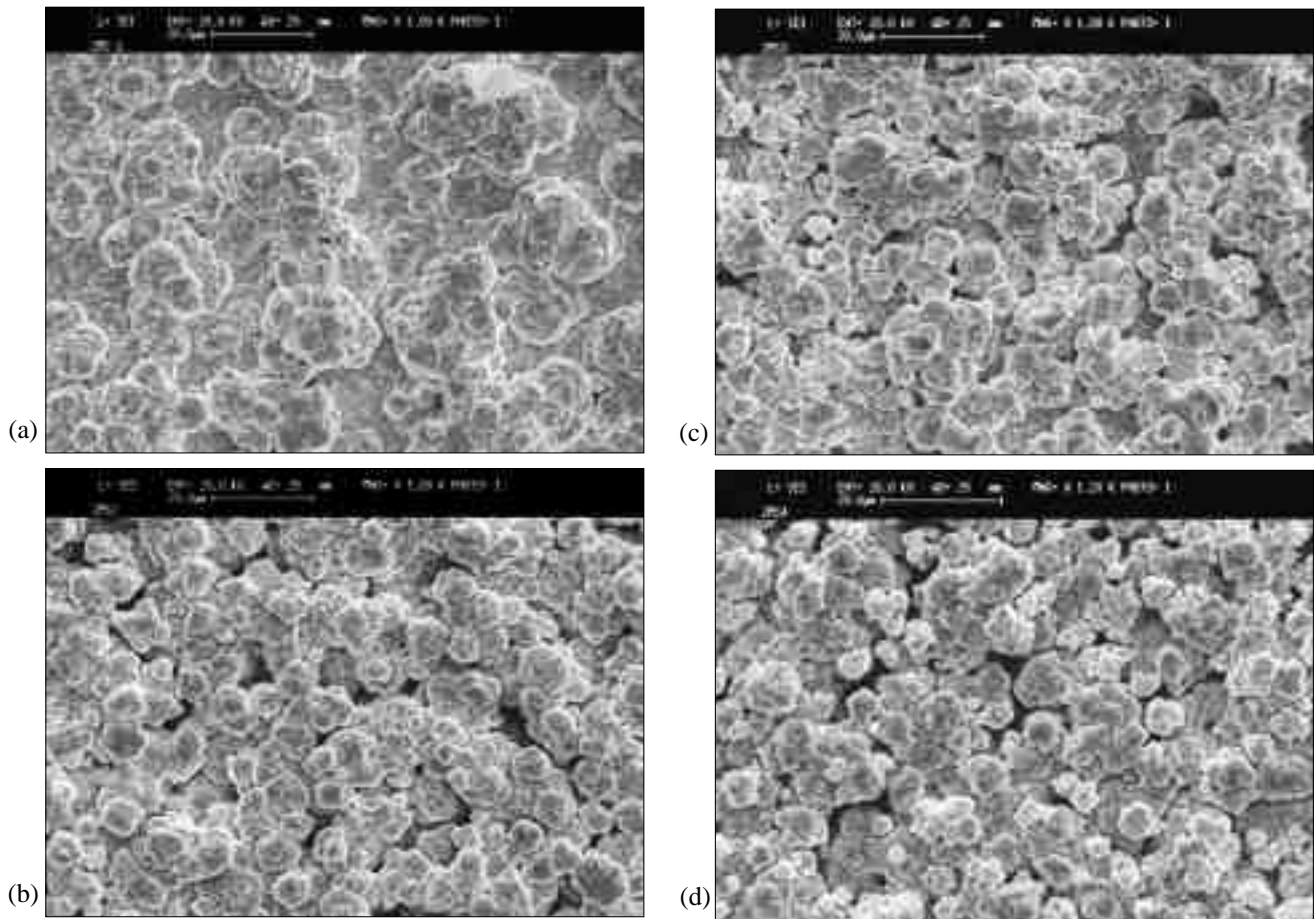


Fig. 4—SEM micrographs of deposits obtained from the bath with no additives: (a) 2 A/dm<sup>2</sup> (20 A/ft<sup>2</sup>); (b) 5 A/dm<sup>2</sup> (50 A/ft<sup>2</sup>); (c) 10 A/dm<sup>2</sup> (100 A/ft<sup>2</sup>); (d) 15 A/dm<sup>2</sup> (150 A/ft<sup>2</sup>).

### Phase Structure of Zn-Mn Alloys as a Function Of Electrodeposition Conditions\*

Presence of Se	Current density, A/dm <sup>2</sup>	Deposition time, min	Phase structure
—	2	60	<u>Zn</u> + ε
—	5	24	<u>Zn</u> + ε
—	10	12	Zn + ε
—	15	8	Zn + ε
SeO <sub>4</sub> <sup>=</sup>	2	60	Zn
SeO <sub>4</sub> <sup>=</sup>	5	24	Zn + (ε)
SeO <sub>4</sub> <sup>=</sup>	10	3	ε + β
SeO <sub>4</sub> <sup>=</sup>	10	6	ε + β
SeO <sub>4</sub> <sup>=</sup>	10	9	ε
SeO <sub>4</sub> <sup>=</sup>	10	12	ε + (β)
SeO <sub>4</sub> <sup>=</sup>	15	8	ε + β
SeO <sub>3</sub> <sup>=</sup>	2	60	Zn
SeO <sub>3</sub> <sup>=</sup>	5	24	Zn + (ε)
SeO <sub>3</sub> <sup>=</sup>	10	12	Zn + ε + (β)
SeO <sub>3</sub> <sup>=</sup>	15	8	ε + (β)

\*Major phase content: underlined “\_”; minor phase content: in parentheses “( )”; otherwise comparable phase contents.

(0.8–2.8%). No clear correlation emerged among current density, selenium valence in the additive and the selenium content in the coating. Local EDX analyses showed that high current density regions (dendrites and tops of humps) tended to contain lower amounts of selenium, which is coherent with the thermodynamic nobility of the element. From thermodynamics,<sup>13</sup> selenium was not expected to deposit, since at the relevant pH and cathodic voltage, the stable form was the soluble HSe<sup>-</sup>. Transient cathode alkalization further stabilizes this form against gaseous H<sub>2</sub>Se.

In the coatings electrodeposited from the bath with selenous acid, more selenium was found than in coatings electrodeposited from the bath with ammonium selenate. Nevertheless, it is known that hydrogen, which forms by electrochemical side reactions and by manganese corrosion in the bath, reduces selenous and selenate ions. This chemical action could proceed in parallel with reduction of selenium to HSe<sup>-</sup> at the relevant cathodic potential. Selenium has been reported to be incorporated into the coatings in both Se<sup>0</sup> and Se<sup>=</sup> forms.<sup>14</sup> Selenium additions tend to increase the current efficiency, except at low current densities. Increasing the amount of H<sub>2</sub>SeO<sub>3</sub> in the range 0.05–0.2 g/L increased

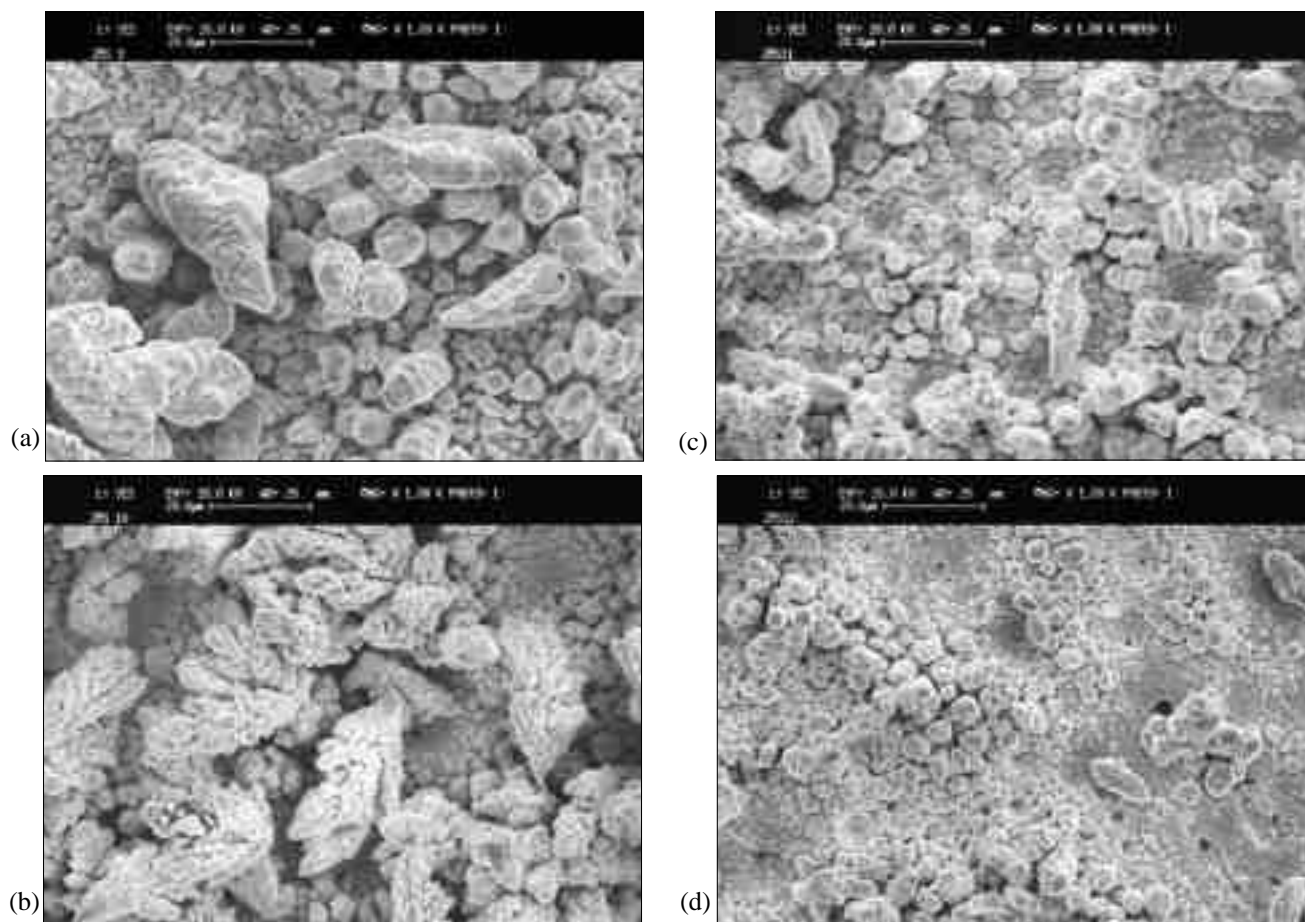


Fig. 5—SEM micrographs of deposits obtained from the bath containing  $\text{SeO}_3^{2-}$ : (a)  $2 \text{ A/dm}^2$  ( $20 \text{ A/ft}^2$ ); (b)  $5 \text{ A/dm}^2$  ( $50 \text{ A/ft}^2$ ); (c)  $10 \text{ A/dm}^2$  ( $100 \text{ A/ft}^2$ ); (d)  $15 \text{ A/dm}^2$  ( $150 \text{ A/ft}^2$ ).

current efficiency, while the effect of progressive amounts of  $(\text{NH}_4)_2\text{SeO}_4$  was not clear, even though the overall increase of current efficiency with respect to the bath not containing selenium compounds was very clear.

The trend of increasing the manganese content with increasing concentrations of either the Se(IV) or Se(VI) compounds was the same for both, but increasing the concentration of  $\text{H}_2\text{SeO}_3$  from 0.05 to 0.20 g/L had limited effect on changing the manganese content in the alloy. Increasing the concentration of  $(\text{NH}_4)_2\text{SeO}_4$  from 0.5 to 1.0 g/L markedly increased the manganese in the alloy. Further additions of ammonium selenate up to 2.0 g/L had no effect on manganese content.

We observed that increasing the concentration of the relevant additives (especially  $\text{H}_2\text{SeO}_3$ ) led to powdered coatings. Further investigations are needed in order to extend our understanding of the specific effects of these two additives.

As far as the variation of manganese content as a function of current density is concerned, the enhancement of manganese content at intermediate and high current densities, expected from altering the competition between zinc deposition and hydrogen evolution, was verified. Even though an overall enhanced hydrogen evolution was expected from selenium-containing baths, the increased cathode efficiency at intermediate and high current densities can be explained in terms of enhanced manganese codeposition. The decrease of current efficiency at the highest current densities was essentially related to powder formation.

The depression of manganese content at low current densities can be explained by an increase of the limiting current density of zinc resulting from the enhanced hydrogen evolution on the zinc-rich cathodes. Manganese codeposition, which takes place according to a regular codeposition mechanism,<sup>8</sup> is therefore delayed. The marked decrease of current efficiency at low current densities is coherent with hydrogen evolution effects on zinc cathodes.

Again, a thorough understanding of the specific effects of the two additives, and in particular the reversed trend of cathode efficiency enhancement versus the increase in additive content, needs further investigation.

### Potentiodynamic Behavior

The polarization effects of ammonium selenate in zinc and Zn-Mn baths are shown in Fig. 2. Polarization curves for a bath similar to the alloy bath, but not containing  $\text{Mn}^{++}$ , show that additions of ammonium selenate in the range 0.5–4.0 g/L have a depolarizing effect whose intensity is related to the amount of additive (Fig. 2a). Variations of selenate concentration had a small effect on the potential (–1060 to –1080 mV) of the limiting cathodic current density inception [ $0.7\text{--}1.1 \text{ A/dm}^2$  ( $7.0\text{--}11.0 \text{ A/ft}^2$ )].

The influence of selenate on the polarization curves for the alloy bath is shown in Fig. 2(b). At low cathodic current densities a rather low depolarization ( $\leq 50 \text{ mV}$ ) was observed. At higher cathodic current densities, polarizing effects (50–100 mV) were observed. Both depolarization (at low current densities) and polarization (at higher current

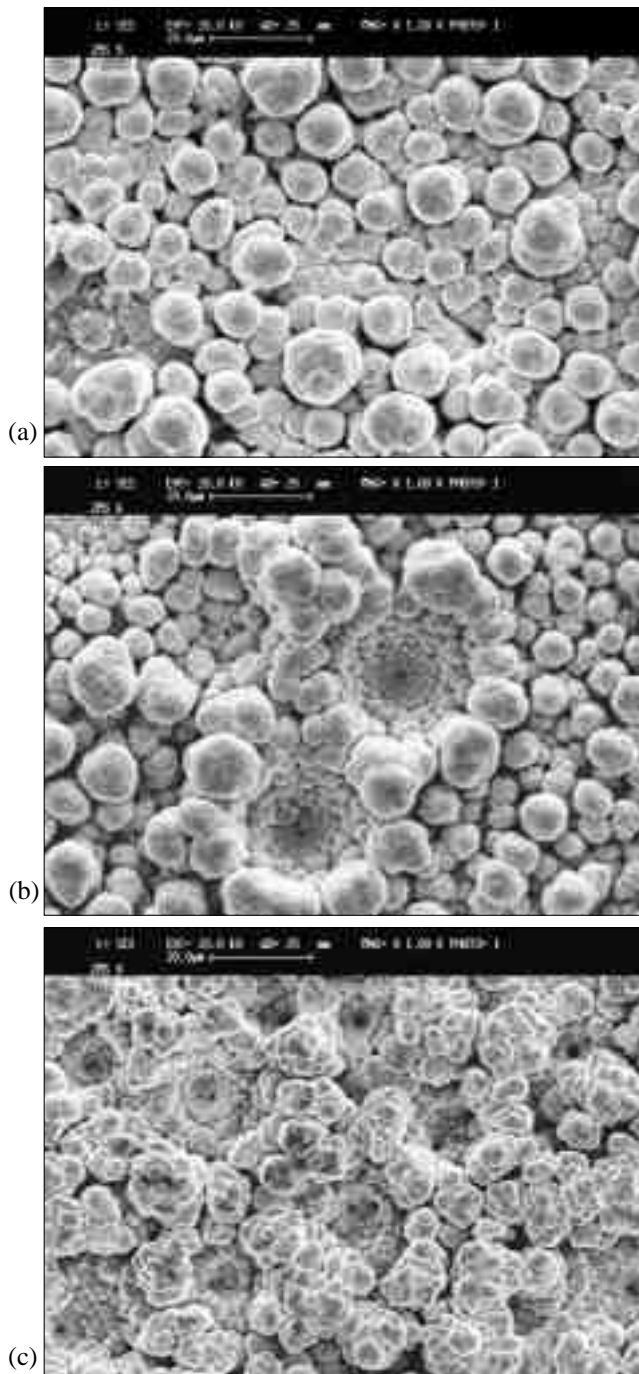


Fig. 6—SEM micrographs of deposits obtained from the bath containing  $\text{SeO}_4^{2-}$ : (a)  $2 \text{ A/dm}^2$  ( $20 \text{ A/ft}^2$ ); (b)  $5 \text{ A/dm}^2$  ( $50 \text{ A/ft}^2$ ); (c)  $10 \text{ A/dm}^2$  ( $100 \text{ A/ft}^2$ ).

densities) effects increased with increasing concentrations of ammonium selenate.

The onset of cathodic passivation could be related to electrocatalytic effects. In any case, the galvanostatic conditions under which all the samples were grown were above this range in a quasi-Tafel region. Further potentiodynamic investigations are being carried out in order to assess the different effects of Se(VI) and Se(IV) compounds on the electrokinetic behavior of the zinc and Zn-Mn systems.

### Crystal Structure

Previous research on the phase structure of the electrodeposited Zn-Mn system<sup>8,15</sup> showed the formation of mixtures of stable

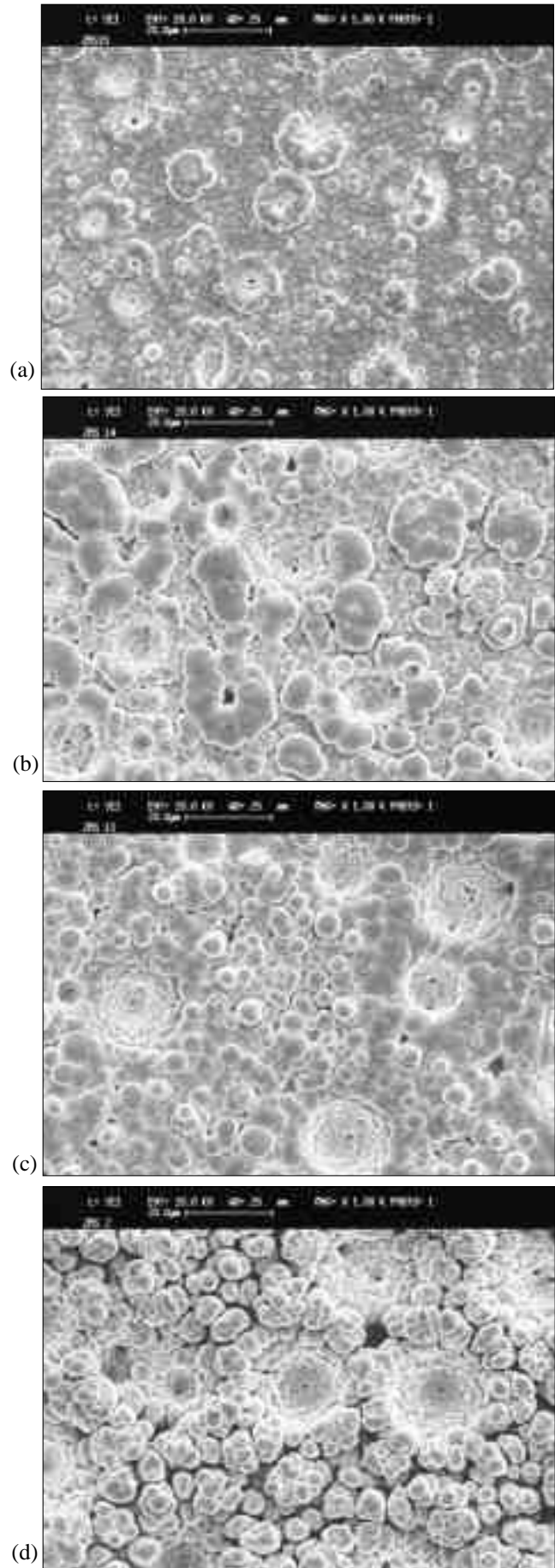


Fig. 7—SEM micrographs of deposits obtained from the bath containing  $\text{SeO}_4^{2-}$  at  $10 \text{ A/dm}^2$  ( $100 \text{ A/ft}^2$ ): (a) 3 min; (b) 6 min; (c) 9 min; (d) 12 min.

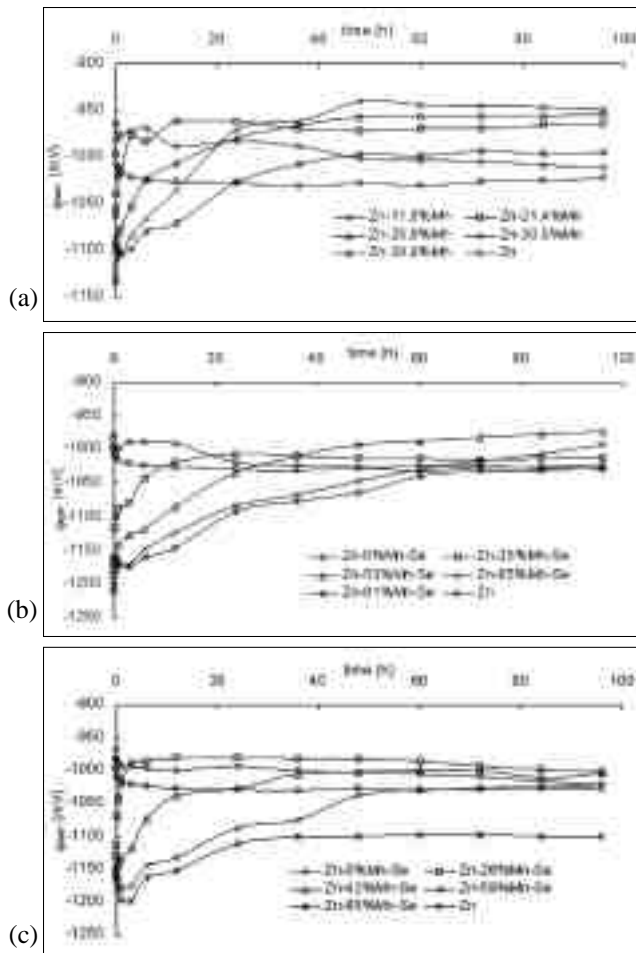


Fig. 8—The dependence of the corrosion potentials on time for ZnMn alloys (in 3% NaCl solution at 18°C): (a) From the basic bath without additives; (b) From the basic bath with 0.05 g/L  $H_2SeO_3$ ; (c) From the basic bath with 0.5 g/L  $(NH_4)_2SeO_4$ .

zinc,  $\gamma$  and metastable  $\epsilon$  and  $\beta$  phases. The structure of alloys deposited from baths with selenium-containing additives were rather similar, as far as the predominance of zinc at lower current densities and the stabilization of  $\epsilon$  at higher ones were concerned. The main difference brought about by the additives is that the  $\gamma$  and  $\beta$  phases were not produced at intermediate current densities. The presence of selenium brought about the appearance of the  $\beta$  phase, which was stabilized at higher current densities. At intermediate current densities [ $\sim 10$  A/dm<sup>2</sup> ( $\sim 100$  A/ft<sup>2</sup>)], the  $\beta$  phase disappeared as deposition proceeded. The phase contents of Zn-Mn alloys deposited from baths containing Se(IV) and Se(VI) are reported, as a function of electrodeposition current density and time, in the table. As far as crystal structure is concerned, no significant differences emerged between the two additives. Typical diffractograms for Zn, Zn +  $\epsilon$ ,  $\epsilon$  and  $\epsilon$  +  $\beta$  phases are shown in Fig. 3.

### Morphology

Previous investigations of the morphology of Zn-Mn<sup>8,16</sup> showed that it generally evolves from plate-like crystals, possibly with elongated platelets, to globular form as current density increases. The typical morphology of pure  $\epsilon$ -phase deposits is strictly globular. As far as samples deposited from the selenium-containing baths are concerned, the following conclusions can be drawn from the surface SEM micrographs.

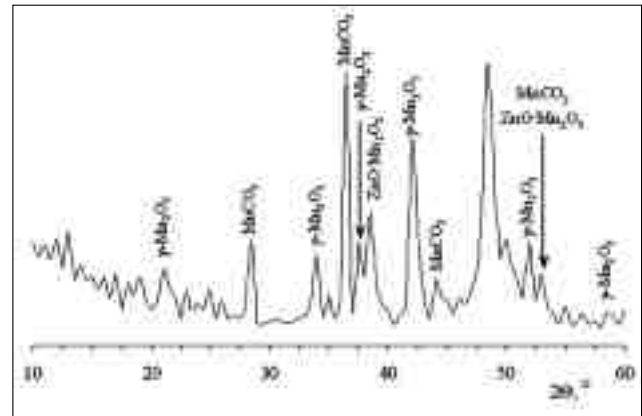


Fig. 9—X-ray diffraction of corrosion products on the surface of Zn-30.5% Mn alloy.

**Baths without selenium.** A clustered “cauliflower” growth was observed (Fig. 4a). The crystallite dimensions were, as expected, reverse-correlated with current density (Fig. 4). Less compact deposits were obtained at higher current densities [Figs. 4(b), (c) and (d)]. The looser morphology of the coatings grown in this study, compared to those in reference 8 may arise from pH differences and details of the concentration of the chemicals in the bath.

**Baths with Se(IV).** Plate-like crystallites were observed at low current densities (Fig. 5a). They progressively changed to globular form as current density was increased—Figs. 5(b), (c) and (d). Hydrogen-bubble holes are visible—Figs. (c) and (d), which is a typical effect of selenium contamination in zinc electrowinning.

**Baths with Se(VI).** The crystallites tended to be globular even at low current densities (Fig. 6a). The globular size was loosely reverse-correlated with current density (Figs. 6 and 7d). Severe hydrogen-bubble effects were observed even at relatively low current densities (Fig. 6b). Nevertheless, the deposit morphologies obtained with  $SeO_4^{2-}$  were much more compact than those obtained with addition of  $SeO_3^{2-}$ .

**Baths with Se(VI): effects of deposition time.** The development of bubble-related morphological instabilities could be followed (*i.e.*, progressive formations of circular globule clusters) if the surfaces of the deposits were observed at different growth times (Fig. 7).

### Corrosion

The measurements of free corrosion potentials of Zn-Mn alloy coatings as a function of time showed a straightforward dependence on the coating composition (Fig. 8). The potentials of zinc and coatings with low (<10%) manganese content were nobler in the initial period and showed a slight decrease of nobility in the course of prolonged immersion. The coatings whose manganese content was in the range of 20–50% were less noble, coherent with the thermodynamic properties of the element. In about 24 to 36 hr however, they became nobler than pure zinc or zinc coatings with low amounts of manganese and selenium.

The data confirmed the results obtained by other studies<sup>16,17</sup> which disclosed the phenomenon of the passivation of high-manganese Zn-Mn alloys. As far as the higher-manganese coatings are concerned, the initial behavior was typical of high-manganese Zn-Mn alloys, but the asymptotic potential they achieved was less noble than that for lower-manganese alloys. This exception was related to the defective morphology of the coatings plated at high current densities. The coatings were not mechanically sound and tended to lose the projecting

high-manganese particles (tending towards dendritic growth) leaving behind the manganese-depleted but smoother underlayer. The effect of selenium additions on a more noble immersion potential was therefore linked to the increased amount of codeposited manganese.

From immersion potential transients, the time of formation of the passivating layer could be estimated as the time of achievement of the asymptotic conditions, which was loosely correlated with manganese content and ranged from about 30 to 60 hr. Faster passivation times seemed to be related to the use of Se(VI) compounds. Further investigations are planned to assess these data in a quantitative way and to investigate relevant film formation mechanisms. Faster formation of passivating layers under anodic conditions can be expected from potentiodynamic data on similar alloys.<sup>17</sup>

X-ray analysis of the corrosion products on zinc-manganese alloy coatings have also been carried out. They contained  $\gamma$ - $Mn_2O_3$ ,  $MnCO_3$  and  $ZnMn_2O_4$  ( $ZnO \cdot Mn_2O_3$ ) (Fig. 9). Previous work on similar systems, based on XPS, only revealed the presence of  $Mn_2O_3$ .<sup>16</sup>

## Conclusions

1. The addition of selenous acid and ammonium selenate into sulfate-citrate baths considerably changes the electrodeposition process of Zn-Mn alloy. Both additives enhance the current efficiency at intermediate and high current densities. The use of selenium-containing additives enables the deposition of high-manganese alloys at low current densities. The presence of trace amounts of selenium in Zn-Mn alloys are related to the reduction of selenous and selenate ions by hydrogen, which forms by cathodic reaction and by the corrosion of plated manganese in the bath.
2. The main difference between the structure of Zn-Mn alloys electrodeposited from the basic bath with and without selenium-containing additives is observed at intermediate current densities. From the bath without additives,  $\gamma$  and  $\beta$  phases are not produced. The presence of selenium leads to the appearance of the  $\beta$  phase, which is stabilized at higher current densities.
3. The presence of selenium compounds influences the morphology of Zn-Mn alloy coatings. Typical plate-like and globular crystallites are observed as well as marked hydrogen-bubble effects.
4. The influence of selenium additives on changes of immersion potentials is related to the high manganese content in the alloy deposits. Passivation of the alloy surface takes place by formation of  $Mn_2O_3$ . Formation times depend on the morphology of the coatings.

## References

1. G.D. Wilcox & B. Petersen, *Trans IMF*, **75**, 115 (January 1997).
2. N. Boschkov, K. Petrov, S. Nikolova, & S.S. Vitkova, *MetallOberfläche* **52**, 514 (July 1998).
3. M. Selvam & S. Gruviah, *Bull. of Electrochemistry* **5**, 352 (May 1989).
4. G. Govindarajan, V. Ramakrishnan, S. Ramamurthi, V. Subramanian & N.V. Parthasaradhy, *Bull. of Electrochemistry* **5**, 422 (June 1989).
5. D.R. Gabe, G.D. Wilcox & A. Jamani, *Metal Finishing* **91**, 34 (August 1993).
6. M. Eyraud, A. Garnier, F. Manzeron & J. Crousier, *Plating & Surface Finishing*, **82**, 63 (February 1995).

7. M. Sagiya, T. Urakawa, T. Adaniya, T. Hara & Y. Fukuda, *Plating & Surface Finishing*, **74**, 77 (November 1987).
8. B. Bozzini, F. Pavan, G. Bollini, P.L. Cavallotti, *Trans IMF*, **75**, 175 (May 1997).
9. A. Sulcius, *Chemija*, **2**, 64 (1996).
10. Y. Sugimoto, T. Urakawa & M. Sagiya, *Ext. Abst. 179th Electrochem. Soc. Meeting, Washington DC, USA*, **91**, 831 (1991).
11. B. Bozzini, F. Pavan, V. Accardi & P.L. Cavallotti, *Metal Finishing*, **97**, 33 (May 1999).
12. D.J. Mackinnon, R.M. Morrison, J.M. Brannen, *J. Appl. Electrochem.*, **16**, 53 (1986).
13. M. Pourbaix, *Atlas d'Equilibres Electrochimiques*, Gauthier-Villars, Paris (1963).
14. J. Janickis, P. Viskelis & A. Suliakas, *LTSR MA darbai, B s.*, **3(142)**, 18 (1984).
15. B. Bozzini, P.L. Cavallotti & F. Pavan, *J. Chim. Physique*, **94**, 1009 (1997).
16. B. Bozzini, P.L. Cavallotti & F. Pavan, *Il Vuoto*, **26**, II, 24 (1997).
17. B. Bozzini, P.L. Cavallotti & F. Pavan, *Atti 26° Conv. Naz. AIM, 6-8/11/1996, Milano (I), Vol. 2, 1996*; p. 9.

## About the Authors



Bozzini



Griskonis



Sulcius

*Prof. Benedetto Bozzini is Professor of Applied Physical Chemistry at the University of Lecce, in Lecce, Italy. He is head of the Surface Engineering Group at the University of Lecce. His main research interests are in metal electrochemistry, including alloy and composite plating, wear and corrosion.*

*Egidijus Griskonis is a PhD student in chemical engineering at Kaunas University of Technology, in Kaunas, Lithuania. He received his MS in chemistry from Vilnius Pedagogical University, in Vilnius, Lithuania. His main research activities are in the study of the electrodeposition and corrosion of zinc-manganese alloys.*

*Dr. Algirdas Sulcius is head of the Department of General Chemistry at Kaunas University of Technology, in Kaunas, Lithuania. His scientific interests are the electrodeposition of manganese alloy coatings, and the investigation of their corrosion properties.*

*Prof. Pietro Luigi Cavallotti is a Full Professor of Metal Science at the Politecnico di Milano, in Milan, Italy. He is president of the European Academy of Surface Finishing and president of the Italian Surface Finishing Association. His main research interests are in the electrodeposition of materials for electronic applications.*